PAPER • OPEN ACCESS

Investigation of properties of nanobridge Josephson junctions and superconducting tracks fabricated by FIB

To cite this article: B Li *et al* 2018 *J. Phys.: Conf. Ser.* **964** 012004

View the article online for updates and enhancements.

IOP ebooks™

Bringing you innovative digital publishing with leading voices to create your essential collection of books in STEM research.

Start exploring the collection - download the first chapter of every title for free.

Investigation of properties of nanobridge Josephson junctions and superconducting tracks fabricated by FIB

B Li[1,2], T Godfrey[1,3], D Cox[1,2], T Li[1,3], J Gallop[1], S Galer[1], A Nisbet[2], Ed Romans[1,3] and L Hao[1]

[1]National Physical Laboratory, Hampton Rd., Teddington TW11 0LW, UK2
[2]University of Surrey, Guildford, Surrey GU2 7XH, UK
[3]London Centre for Nanotechnology, University College London, WC1H 0AH, UK

E-mail: ling.hao@npl.co.uk

Abstract. An important requirement across a range of sensitive detectors is to determine accurately the energy deposited by the impact of a particle in a small volume. The particle may be anything from a visible photon through to an X-ray or massive charged particle. We have been developing nanobridge Josephson junctions based SQUIDs and nanoSQUID devices covering the entire range of particle detection energies from 1eV to MeV. In this paper we discuss some developments in nanobridge Josephson junctions fabrication using focussed ion beam (FIB) and how these developments impact future applications. We focus on tuning of the transition temperature of a superconducting thin-film absorber, with the aim to match the absorber T_c to the working temperature range of the SQUID and also on using a new Xe FIB to improve Josephson junction and superconducting film quality.

1. Inductive transition edge detector

The bolometer systems we are developing are based on an inductive superconducting transition edge detector (ISTED). The basic principle [1] is that a superconducting thin film absorber is deposited within the loop of a micrometre-scale planar SQUID [2]. Figure 1 shows an SEM image of a square loop SQUID with two nanobridge Josephson junctions, with a thin film Nb absorber deposited within the SQUID loop. The absorber is selected so that it has a lower transition temperature T_c than the SQUID. If the temperature of the chip is adjusted so that both the SQUID is in its optimum operating range and the absorber is just below its own transition temperature, the absorber is in the regime where the superconducting penetration depth (λ) is a very sensitive function of temperature. If the absorber receives some energy input from an incident energetic particle the energy deposited in it will raise its temperature, thus increasing the superconducting penetration depth and resulting in a change in the effective area of the SQUID loop. If the SQUID is biased with an offset flux the change in flux periodicity will result in a large change of SQUID output voltage, even for a change in temperature as small as 1μK.

The superconducting thin-film absorber layer can be seen as a transducer, converting the thermal energy signal into magnetic flux change, which is detected by the surrounding SQUID as a pulse in its voltage output. Unlike conventional superconducting transition edge sensors (TES) [3], the ISTED absorber is not biased into the normal state, remaining permanently superconducting so that the system is not subject to Nyquist noise, thereby improving its overall energy sensitivity. By adding to the

absorber a further thin layer of a material (such as amorphous carbon or graphene) an ISTED can be converted to a microbolometer or a micro/nanodosimeter [4], where the absorbing layer is selected for thickness and other properties to optimize response for the chosen application. Once an incident event happens, the energy released will be absorbed by the absorber, resulting in a pulse signal of the output voltage. The magnitude of the pulse signal quantitatively reflects the energy released in this event.
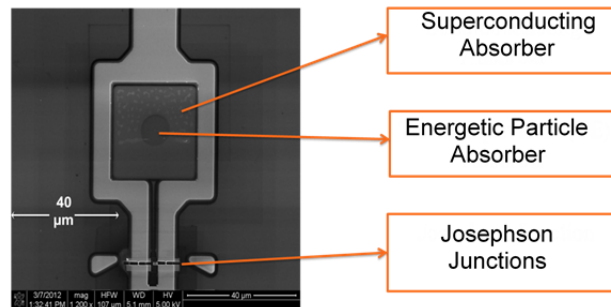

Figure 1. An SEM image of a prototype micron-scale ISTED device with tissue-equivalent absorber aimed for micro/nano dosimetry.

2. Tuning the SQUID-Absorber Transition Temperature

For optimal performance of the ISTED calorimeter the T_c of the absorber film should be slightly lower (typically 1K) than the T_c of the SQUID itself. This means that the Nb nanobridge SQUID which is usually operated at around 2K below the T_c of pure Nb has an absorber which is still superconducting at the SQUID operating temperature but remains in the region where its penetration depth is still strongly temperature dependent. We have investigated two different methods to 'tune' the T_c of the absorber film. The first involves exposure to a scanning Gallium (Ga) FIB of which the amount of Ga ions deposited into a unit area of the Nb film can be easily and precisely controlled. Of course this process not only leads to reduction of the film thickness but also causes damage to the thin film's crystal lattice and implantation of Ga ions. After a selected number of passes, corresponding to specific exposure, the T_c of the film is re-measured then the process is repeated. Another technique for tuning the T_c of a film is to control the thickness during the deposition of the film. We have deposited Nb films with different thicknesses and measured the transition temperature. The first method, by FIB dosing and milling, only requires a single deposition and fabrication step for both SQUID and absorber. The second method, controlling the deposited thickness of the absorber, requires separate Nb deposition and patterning steps, but may provide greater control over T_c. The two methods are described below.

2.1. Gallium ion dosing and milling
When energetic ions impinge on a sample surface there are two pronounced effects. Firstly, the ion implants into the sample causing a cascade of damage as it loses energy before coming to rest. Second, if sufficient energy to overcome the binding energy of surface atoms is released by the ion, sample atoms can be ejected in a process known as sputtering [5]. FIB instruments with Ga (and more recently Xe) ion sources exploit this latter phenomena, and are now well established tools in semiconductor and wider material science applications. Less well known is that FIBs can also be used as fabrication and sample modification tools. We use this technique to fabricate nano-SQUID devices where that Ga FIB modifies simple Nb films to produce extremely low noise SQUIDs in a fast two stage process. In these devices the SQUID nanoscale junctions are of the nanobridge where the FIB is used to mill away the film to produce a narrow junction region with suppressed T_c.

Using a similar mechanism to Nb film ion milling, but additionally relying on the Ga ion dosing, a FIB instrument can also be used to tune the T_c of a Nb film. The Nb films were sputter-deposited on a silicon substrate with a very thin Ti adhesion layer and total thickness in the range of 195-200 nm. A four-terminal lead and bond pad arrangement was used to allow the T_c of the film to be measured. The

films were exposed with the ion beam across the full width of a track (10 μm) over a length of 3 μm and for a range of ion doses (see Fig.2). Using a 30 kV, 100 pA beam current, with beam step of 10 nm in both x and y direction, and a 1 μs beam dwell at each point gave a dose of 6.2 ions/nm^2 for a single pass of the beam. This dose was repeated in sets of 25 identical passes giving approximately 155 ion/nm^2 per set, up to a maximum of 700 sets. After a certain amount of dose, resistance of the Nb film is measured as a function of temperature and T_c of the dosed Nb film is plotted versus the number of Ga ion beam passes in Figure 3. T_c decreases from 8 K to 4.3 K as the Ga beam pass increases from 100 to 400. The superconductivity of the Nb film is fully destroyed beyond 500 passes.
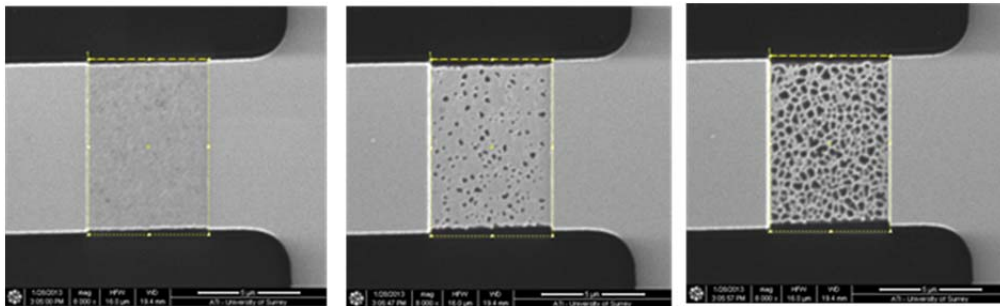

Figure 2. Scanning ion images of Nb film following different levels of ion exposure (corresponding to 100 passes, 400 passes and 600 passes) of Ga ion beams of 30 keV, and beam current ~100 pA. Total removal film is achieved with total ion flux of $4.34 \times 10^9/\mu m^2$. Effects of ion channelling can also be seen. The exposed area is denoted by the yellow dashed box.
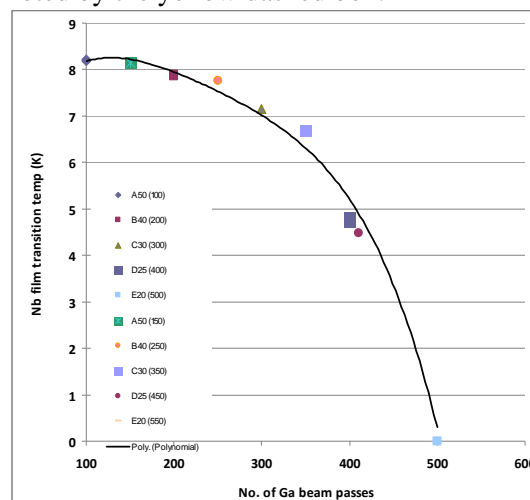

Figure 3. The T_c of the Nb film vs. the No. of Ga ion beam passes. The data is from several different Nb film with an initial thickness of 200 nm. The thickness of film removed in each beam pass is approximately 0.28nm. The solid line shows a third order polynomial fit to the data.

Owing to the importance of ion beam implantation in the semiconductor industry, considerable modelling of ion beam damage and sputtering has been carried out at many levels of sophistication, ranging from molecular dynamics models of single (and few) ion collisions in specific orientations of single-crystals [6], to Monte-Carlo and numerical models approximating to 'bulk' conditions, with ion doses at the upper end of the range offered by FIB milling (>> 10^9 ions/m^2). When considering deposited thin metal films, such as Nb, irradiated with a Ga ion beam, a model of the latter type is more appropriate, as the number of ions can be very large and the samples can be considered as 'bulk' in nature. The main advantages of these 'bulk' models is that at least two of them are offered as readily available, free to use, software packages [7]. Furthermore, in the case of the numerical solution

offered by the SUSPRE package it is very rapid and extremely simple to use. The Ga implant profile after one set of 25 repeat passes predicted by the SUSPRE software is shown in Figure 4. As can be seen the predicted profile shows a peak concentration of approximately 15 % Ga, 12nm from the sample surface with a long Gaussian tail extending 40nm into the Nb film. Also the predicted damage profile (not shown) for this dose largely mirrors the implant profile and shows 100% amorphisation just beyond the peak implant concentration. Simulating further repeated passes of the beam at the stated dose shows the damage profile ultimately extending to the full range of the implant (40 nm) with 100% amorphisation after just over 100 repeat passes. Along with the damage profile and implantation range SUSPRE also calculates the expected sputter yield (in Nb atoms per Ga ion) and once again this is in good agreement with SRIM. The predicted yield is almost 3.8 Nb atoms per Ga ion (at 30 kV and normal incidence).

Turning to the actual ion milling, under the stated dose conditions that it takes approximately 700 repeat passes of the beam to fully remove the Nb film to Si substrate. Assuming no change in milling rate this is approximately 0.28 nm of material removed per pass of the beam and with the lattice parameter of Nb being 0.33 nm this approximates to one atomic layer per repeat pass. The model prediction for sputter yield and with a dose of 6.3 ion/nm^2 would give a removal rate of 0.4nm per pass. With the atomic density of Nb approximately 55 atoms per cubic nm and a removal rate of 0.28nm per repeat, the actual sputter yield is therefore 2.5 Nb atoms per Ga ion, only 65% of the calculated rate.
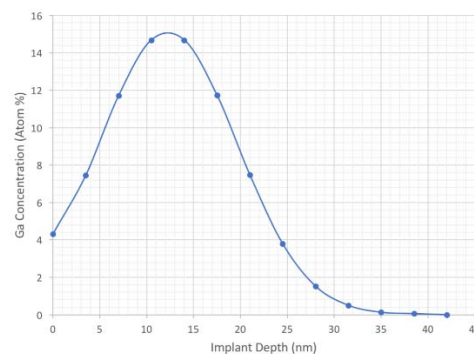

Figure 4. Calculated Ga implant profile for a 30 kV Ga ion dose of approximately 155 ions/nm^2 in Nb.

Assuming a uniform material removal rate, after 200 repeats of the dose the film is thinned by approximately 56 nm. The ion-cascade damaged region would have moved inward into the film uniformly as the film is thinned and with projected range of damage of at least 40nm this would still leave 100 nm of undamaged Nb film. This is the first dose level where we observe a slight suppression in the T_c of the film (Figure 3). Beyond this we see a steady fall in T_c as the film is increasingly dosed to 350 repeats, corresponding to the point the film is approximately half thickness. Allowing for the ion-damaged zone, the undamaged portion of film at this point would be of the order of 60nm thick. Beyond this point further dosing of the film causes a rapid decline in T_c with a further 100 repeat doses causing a larger fall in T_c than the previous 350. At this point the pristine film is approximated to be only 34nm in thickness with any further dosing causing a complete loss of T_c.

2.2. Use of Xe Focussed Ion Beam

Recently we have been able to test a different FIB system which uses Xe as the massive ion to provide milling. The potential advantages over a conventional Ga ion beam are that the inert gas will not lead to modified electronic properties of the underlying Nb film since, unlike Ga, the Xe will not form chemical modification of the film through alloying. In addition local electronic doping of the film should be reduced. In other respects the mechanical effects of both Ga and Xe should be similar, in terms of milling rate and damage to the upper un-milled surface layers. The Xe mass is significantly

higher than the Ga ion mass which should also somewhat increase the milling rate. We have produced a number of Xe milled Nb nanoSQUIDs based nanobridge junctions and their properties are at least as good as similar Ga devices (see an example I-V curves ad function of the magnetic fields in fig 5).
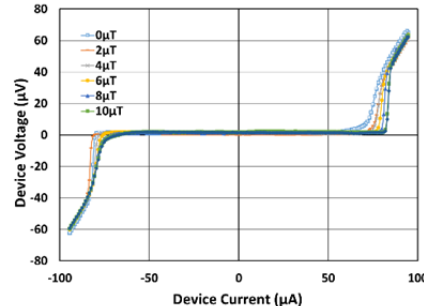

Figure 5. A series of current-voltage curves are shown with a range of magnetic fields.

2.3. *Control of the thickness of the absorber*
A second approach has been investigated as a means of controlling the T_c of a Nb film absorber, to tune it to the optimum operating temperature. Key is that the T_c of a pristine Nb thin film is strongly related to its thickness [8], especially when the thickness is less than 30 nm, allowing the T_c to be tuned by controlling its thickness. In such an approach, the absorber is deposited *after* the fabrication of the SQUID, in a routine lift-off process followed by EBL patterning. The sputtered Nb film thickness is controlled by the sputtering time. The T_c versus thickness relationship is highly dependent on the deposition system and operating conditions. To find out the true thickness of the film with desired T_c, we have deposited several Nb films with different thickness on silicon substrates, and measured the resistance of a patterned track of these films as a function of temperature in a four-probe configuration. In Figure 6 we plot the T_c and corresponding thickness (measured by a Dektak XT surface profiler) of resistance of a patterned track of these films as a function of temperature in a four-probe configuration. Note the T_c increases rapidly with film thickness in the range from 20 nm to 35 nm, which shows in the plot, the trend of T_c as a function of the thickness can be well fitted in a proximity effect model [9, 10]. Since Nb is easily oxidised in air thin Nb films are usually covered by an oxide layer of several nanometres thickness, which can be regarded as normal metal. Due to the existence of such a normal metal layer, the T_c of the Nb film is suppressed by the superconducting proximity effect. The extent of the suppression depends on the thickness ratio of normal layer and superconducting layer.

If we assume the thickness of oxide layer and superconducting layer are *a* and *d* respectively, the T_c of such a two-layer film can be predicted by the relationship

$$T_c = T_{c0} \left(\frac{1.13 \Theta_D}{T_{c0}} \right)^{-\frac{N_N(0)}{N_S(0)} \frac{a}{d}}$$

where T_{c0} is the transition temperature of bulk Nb (9.3 K), Θ_D is the Debye temperature of Nb (275 K), and $N_N(0)$ and $N_S(0)$ are the density of states for normal and superconducting layers, respectively. Thus, the thinner the Nb film, the larger the thickness ratio of normal layer and superconducting layer, and therefore the lower the transition temperature T_c.

3. Conclusion and Future Work
The extremely high sensitivity and ultra-low noise performance of nanobridge Josephson junctions make them ideal for fabricating ISTEDs, which can be used to detect rather small energy absorption [11,12]. This makes it practical to try to understand the processes by which the transition temperature of a superconducting thin film may be adjusted for optimal performance, whether it is for SQUIDs/nanoSQUID operation or for tuning the operating temperature of a superconducting absorber. We have been pursuing two distinct methods which have been described in this paper. It is already clear that both are able to provide relatively reproducible changes in T_c, (up to at least 3.5K), whether

by means of implantation of ions and damage or by the suppression of T_c by the presence of an underlying normal metal film. Each method will have advantages in different situations.
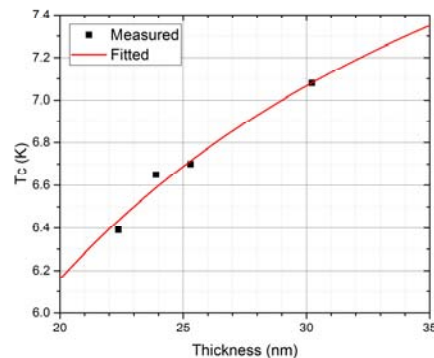

Figure 6. The transition temperature T_c versus the thickness of Nb films. The black dots are measured data and the red curve is fitted by the proximity effect model discussed in the main text.

In parallel with this investigation we have also proceeded to test combined SQUID and absorber designs for prototype ISTED micro/nanodosimeters. The devices will be tested in a cryogen-free pulse tube cooler system with horizontal beam access, to allow a charged particle beam to access the absorber with minimal energy absorption in the mylar windows which support the vacuum necessary for the cryogenic environment. The first beam measurements using the micro-beamline at the National Ion Beam Centre at Surrey University are expected in future. We have also begun investigating the microwave capabilities of these devices, showing that they are likely to be suitable for microwave readout techniques and microwave circuit applications. Microwave reflectometry measurements on inductively coupled SQUIDs are proving to be an advantageous technique for high sensitivity operation. Reflectometry would allow us to make measurements at even higher sensitivity than currently available with microwave inductive readout Johnson noise sources in the junctions will be much reduced.

References
[1]   Hao L, Macfarlane J, Josephs-Franks P and Gallop J 2003 *IEEE Trans. Appl. Supercond.* **13**, 622
[2]   Granata C and Vettoliere A 2016 *Physics Reports* **614** 1-69
[3]   Irwin K D and Hilton G C 2005 *Topics Appl. Phys.* **99** 63–150
[4]   Furetta C, Prokic M, Salamon R, Prokic V and Kitis G 2001 *Physics Research Section A:* **456** 411-417
[5]   Cox D C, Gallop J C and Hao L 2014 *Nanofabrication* **1** 53-64
[6]   Yamamura Y and Takeuchi W 1987 *Nuclear Instruments and Methods in Physics Research Section B: Beam Interactions with Materials and Atoms* **29** 461-470
[7]   www.srim.org
[8]   Bose S, Raychaudhuri P, Banerjee R, Vasa P and Ayyub P 2005 *Phys Rev. Lett.* **95** 147003
[9]   Frommberger M, Mattiocco F, Sabon P, Schicke M, Schuster K F and Laborde O 2000 *Proc. 11th Int. Symp. on Space Terahertz Technology*
[10]   McMillan W L 1968 *Physical Review* **175** 537
[11]   Hao L 2011 *J. Phys.: Conf. Ser.* **286** 012013
[12]   J Gallop J, Cox D and Hao L 2015 *Supercond. Sci. Technol.* **28** 084002